

Journal of Materials Chemistry B

Accepted Manuscript



This is an *Accepted Manuscript*, which has been through the Royal Society of Chemistry peer review process and has been accepted for publication.

Accepted Manuscripts are published online shortly after acceptance, before technical editing, formatting and proof reading. Using this free service, authors can make their results available to the community, in citable form, before we publish the edited article. We will replace this *Accepted Manuscript* with the edited and formatted *Advance Article* as soon as it is available.

You can find more information about *Accepted Manuscripts* in the [Information for Authors](#).

Please note that technical editing may introduce minor changes to the text and/or graphics, which may alter content. The journal's standard [Terms & Conditions](#) and the [Ethical guidelines](#) still apply. In no event shall the Royal Society of Chemistry be held responsible for any errors or omissions in this *Accepted Manuscript* or any consequences arising from the use of any information it contains.

Cite this: DOI: 10.1039/c0xx00000x

www.rsc.org/xxxxxx

ARTICLE TYPE

Synthesis of Amphiphilic Reduced Graphene Oxide with Enhanced Charge Injection Capacity for Electrical Stimulation of Neural Cells

Qi Zhang^{a,b}, Jun Xu^c, Qin Song^c, Ning Li^c, Zhaolei Zhang^a, Kunyang Li^a, Yuyang Du^c, Liqiong Wu^c, Mingliang Tang^c, Liwei Liu^c, Guosheng Cheng^{*c} and Jian Liu^{*a}

^aJiangsu Key Laboratory for Carbon-Based Functional Materials and Devices, Institute of Functional Nano and Soft Materials (FUNSOM), Collaborative Innovation Center of Suzhou Nano Science and Technology, Soochow University, Suzhou, Jiangsu 215123, China. E-mail: jliu@suda.edu.cn

^bState Key Laboratory of Molecular Engineering of Polymers, Fudan University, Shanghai 200433, China.

^cSuzhou Institute of Nano-Tech and Nano-Bionics, Chinese Academy of Sciences, 398 Ruoshui Road, Suzhou Industrial Park, Jiangsu 215123, China. E-mail: gscheng2006@sinano.ac.cn

Received (in XXX, XXX) Xth XXXXXXXXXX 20XX, Accepted Xth XXXXXXXXXX 20XX

DOI: 10.1039/b000000x

Advanced neural research demands new electrode materials with high performance. Herein, we have developed a facile approach to synthesize amphiphilic reduced graphene oxide (rGO) and demonstrated its performance in electrically stimulating neural cells with high charge injection capacity. Synthesis of the amphiphilic rGO is featured with covalent functionalization and simultaneous thermal reduction in a one-step manner. The covalent functionalization of methoxy poly(ethylene glycol) (mPEG) chains on rGO surface not only provides the high dispersibility in various solvents enabling convenient post-treatment processes, but also allows for an enhancement in double-layer charging capacitance. Calcium imaging of PC12 neural cells on the amphiphilic mPEG-rGO films has revealed a predominant increase of cell percentage with higher action potentials, derived from double-layer capacitance enhancement in charge injection. These results suggest that the new material of amphiphilic mPEG-rGO is capable of providing much safe and efficacious solution for neural prostheses applications.

Introduction

Electrical stimulation of neural cells is widely employed in emerging technologies for prostheses and medical treatments of spinal cord injury, stroke, sensory deficits, and neurological disorders¹. The development of electrode materials is one of the critical factors because they interface the neural cells with the physical facilities. An ideal candidate of electrode materials needs to be safe and biocompatible in the first place, and efficient in mediating the charge transfer from electron flow in the electrode to ion flow in the cells². The charge injection can be conducted by capacitive effect involving the charging and discharging of double layer at the electrode-electrolyte interface, or faradaic reaction in which surface-confined species are oxidized and reduced³. Although faradaic reaction may provide higher current density, the method is accompanied by the generation of complicated chemical species unfriendly to the biological cells in many cases. Therefore, capacitive charge injection is in principle a more desirable approach than faradaic reaction⁴.

Recent development in carbon nanomaterials offers new opportunities to design stimulation electrodes with high capacitive charge injection capability^{2,5}. Graphene, single or few-layered two-dimensional (2D) sp²-bonded carbon sheet, has been widely explored for adoption in electronic and optoelectronic devices⁶, heat storage⁷, photodynamic therapy⁸ and sensors⁹. Compared with conventional inert electrode materials (e.g.

platinum), the unique properties of graphene make it an excellent candidate to address the requirements for advanced neural research. (1) biocompatibility and bioactivity. It was reported that graphene can promote neurite of hippocampal cells sprouting and outgrowth^{10,11} and induce stem cells to preferentially differentiate into specific lineages¹²⁻¹⁴. Moreover, owing to its strong noncovalent interactions with biomolecules, graphene can act as a substrate to preconcentrate the biomolecules for regulation of cell behavior and fate¹⁵⁻¹⁷. (2) mechanical compliance with the neural tissues. For example, in-plane Young's modulus of monolayer graphene is around 1 TPa, about five times stronger than steel¹⁸. Yet graphene can be bent to large angles without breaking and variation in electric resistance¹⁹. This combination of strength and flexibility is highly desirable for robust and stretchable electrodes in neural prostheses. (3) Electrical conductivity. The graphene has been proven to possess high conductivity for charge transport and enable efficient electron transfer from electrode surface to the electrolyte²⁰. However, few studies involved the electrical stimulation of neural cells on graphene platforms²¹, leaving scarcely any data about the effect of surface functionalization on the charge injection capability as well as the consequence of neural cell behaviors.

In this work, we developed a facile one-step method to synthesize amphiphilic reduced graphene oxide (rGO) for application of neural prosthesis materials. The amphiphilic functionalization of rGO surface with poly(ethylene glycol) (mPEG) not only provided a high dispersibility in various solvents enabling convenient post-treatment processes, but also

offered an enhanced double-layer charging capacitance. Moreover, a proof-of-concept study was conducted on the amphiphilic mPEG-rGO film as a conductive platform for electrical stimulation of pheochromocytoma (PC12) neural cells (a model cell system for varieties of neural functions). Calcium imaging of PC12 neural cells on amphiphilic mPEG-rGO films revealed that the percentage of the cells with higher action potentials increased significantly, contributed by the effect of double-layer capacitance enhancement for charge injection. These results suggested important applications of the amphiphilic mPEG-rGO for neural prostheses featured with high effectiveness and biosafety.

Experimental

Preparation of rGO

The yellow brown GO was prepared from natural graphite powder (300 mesh, Alfa Aesar) by a modified Hummers method^{22,23}. Hexamethylene diisocyanate (HMDI)-activated methoxy poly(ethylene glycol) 5000 (A-mPEG 5k, see Fig. S1 in Supporting Information) was synthesized according to the previous reported protocols²⁴. The mPEG-rGO was accomplished by a so-called one-step synthesis method. In briefly, anhydrous graphene oxide foams (10 mg) were added into a 25-mL round-bottom flask equipped with a magnetic stir bar, followed by addition of 10 mL anhydrous *N,N*-dimethylformamide (DMF). The flask was then sonicated for 30 min under nitrogen. The A-mPEG 5k (0.5 g) was next loaded and the mixture was heated at 160 °C with magnetic stirring under nitrogen for 1-5 h. The product was centrifugated, washed with DMF and ethanol for six times. The control was obtained by substitution of A-mPEG 5k to pure mPEG 5k with other conditions unchanged. The rGO_{N2H4} was synthesized by using hydrazine as a reducing agent²⁵ (more details available in Section 2 of Supporting Information). Their powders were obtained by drying the ethanol solution under vacuum. Their films were prepared by filtration of the aqueous solution through 0.25- μ m-pore cellulose membrane, followed by transfer to a solid conductive substrate for cell culture.

Characterization

The morphology and average thickness of films were characterized by repeated atomic force microscopy (AFM) (Digital Instrument Dimension 3100, Veeco). Structural properties of rGOs were measured by X-ray diffraction (XRD) (D8 Advance, Bruker) with a Cu K α source ($\lambda=1.5406$ Å). Fourier transform infrared spectroscopy (FT-IR) spectra were measured by a Nicolet 6700 Fourier transform infrared spectrometer (Thermo) and samples were dispersed in pressed KBr disks. The X-ray photoelectron spectroscopy (XPS) (Axis Ultra DLD, Kratos, UK) was performed by utilizing an Al K α X-ray source operated at 40 eV. The reduction quality was examined by Raman spectrometer (lamRAM HR800, HORIBA, France). Thermogravimetric analysis (TGA) (TG/DTA 6200, Seiko) was performed under a nitrogen flow in a Pt crucible on sample sizes from 2 to 3 mg. The electrochemical experiment was performed with a CHI620c Electrochemical Analyzer (CHI, Austin TX). Glass carbon (GC) electrode ($\Phi=3$ mm) serves as the working electrode, a platinum wire as the auxiliary electrode, and an Ag/AgCl electrode as the reference electrode, respectively.

Culture of PC12 Cells

PC12 cells were cultured in DMEM supplemented with 10% fetal bovine serum, 100 μ g/mL penicillin and 100 μ g/mL streptomycin at 37 °C in a humidified atmosphere with 5% CO₂.

Cell viability assay

Cell viability of mPEG-rGO was evaluated with tissue culture polystyrene (TCPS) as control using LIVE/DEAD[®] viability/cytotoxicity kit for mammalian cells (Invitrogen, USA) according to the manufacturer instructions. Percentage of live cell was calculated by counting the percentage of Calcein-AM positive cells over total cell number. Additionally, the details of 3-(4,5-dimethylthiazol-2-yl)-2,5-diphenyl tetrazolium bromide (MTT) assay were described in Supporting Information. The result was given as the mean \pm standard error of the mean.

Electrical Stimulation & Calcium Imaging

To seed PC12 Cells on the rGO films, a cloning ring (O.D. 10 mm & height 10 mm) was mounted on the substrate. An electrical lead was loaded directly onto the dry area of the graphene substrate by using silver paste and copper wire. The input stimulation was applied with the aid of a function generator (S3K, Grass Technologies, USA) that gave flexibility in the applied electrical stimulus signal. The cells were further stained with Fluo-4 AM dye before stimulation (2.5 μ mol, Dojindo Laboratories, Japan). A series of 1~100 ms monophasic anodic pulses were applied with duration of 10 s. The stimulation potential was limited to lower than 0.6V to avoid undesired effects of faradaic electrolyte reactions. Time-lapse calcium level in live PC12 cells was measured using fluorescence microscopy.

Results and discussion

Scheme 1 illustrates the design and preparation of amphiphilic reduced graphene oxide (rGO) composite coated electrode. The rGO amphiphilic functionalization was achieved by a new method featured with one-step synthesis procedure allowing for tunable material properties. The surface modification was performed by conjugating isocyanate group of A-mPEG 5k with surface hydroxyl functional groups of GO via formation of amides or carbamate esters²⁶. Simultaneously, the GO sheet was thermally reduced during this reaction²⁷. Afterwards, the mPEG chain was covalently immobilized on the carbon surface of rGO to form an amphiphilic outer layer, consequently facilitating the dispersion of mPEG-rGO in both organic low polar and water-miscible high polar solvents. The as-prepared amphiphilic mPEG-rGO was filtered to form a film on cellulose membrane (pore size 0.25 μ m, diameter 47 mm), and then transferred to a conductive substrate for cell culture and electrical stimulation (Section 2 in Supporting Information).

The morphology and structure of mPEG-rGO were studied by tapping-mode AFM. Fig. 1 shows the AFM images and cross-section analyses of a single-layer GO and mPEG-rGO adsorbed on mica, respectively. The thickness of a single layer GO sheet was measured about 1.3 nm, consistent with the previous reports²⁸. The thickness of a single layer of mPEG-rGO sheet was 1.7 nm. Thus, the interlayer distance between mPEG-rGO was enlarged by the intercalated mPEG molecules. Because the procedure of one-step synthesis was performed in a homogeneous solution with steady stirring, it was likely that the mPEG molecules attached onto both sides of rGO sheets, thus forming a sandwich-like structure. The covalent bonding of mPEG

molecules onto GO sheets was further verified by Fourier transform infrared spectroscopy (FT-IR, Fig. S2 in Supporting Information). Upon treatment with A-mPEG 5k, the C=O stretching vibration at 1730 cm^{-1} of GO became obscured by the appearance of a strong absorption peak at 1564 cm^{-1} , ascribed to the stretching vibration of carbamate or amide group. Significantly, the broad and intense peak of O-H ($3200\text{--}3700\text{ cm}^{-1}$) stretching vibration was altered to the N-H stretching vibration at 3345 cm^{-1} , suggesting that the hydrogen-containing functional groups of GO were substituted by mPEG molecules after their reaction with A-mPEG 5k²⁶. Additionally, the signal of isocyanate group (2270 cm^{-1}) was invisible in the spectrum of mPEG-rGO, indicating that the treatment of GO with A-mPEG 5k resulted in chemical reactions and not mere adsorption/intercalation of the unreacted A-mPEG 5k.

To further investigate the structure of mPEG-rGO, UV/Vis absorption spectroscopy, XPS, Raman spectra and TGA were employed in our experiments. The reduction of GO to rGO was monitored by the UV/Vis absorption spectra (Supporting Information, Fig. S3), and further confirmed by the results obtained by XPS (Supporting Information, Fig. S4) and Raman spectra (Supporting Information, Fig. S5). All the data supported that GO was deoxygenated and reduced, and mPEG chains were immobilized on carbon plane. Based on the TGA data (Supporting Information, Fig. S6) and the yield of mPEG-rGO (~120%), it was estimated that mPEG-rGO was comprised of 20–50 wt% of mPEG.

The powder XRD pattern was utilized to investigate the reduction quality of the mPEG-rGO, depicted in Fig. 2a. A typical broad peak near 10.5° (d-spacing $\sim 8.4\text{ \AA}$) was observed for the GO powder. Compared with the parent GO, the peak of mPEG-rGO displayed a dramatic shift to higher 2θ angles with the increase of reaction temperature. The peak of mPEG-rGO reduced at $160\text{ }^\circ\text{C}$ was finally increased to 23.5° (d-spacing $\sim 3.8\text{ \AA}$), very close to that of rGO reduced by hydrazine (rGO_{N₂H₄}). The result suggested that rGO was well ordered with two-dimensional sheets although part of graphene plane was occupied by the coupled mPEG chains. Additionally, the reaction process was monitored using XRD. As shown in Fig. S7 (Supporting Information), the peak of GO (10.5°) quickly right-shifted to 23.4° , suggesting that the electronic conjugation within the graphene sheets was recovered during reduction. There was little further increase of peak position after 1 hour, indicating completion of the reduction. This experiment also indicated that the electrical and polymer conjugation level of graphene was chemically controllable, thus providing possibilities to tune the optical and electrical properties of graphene sheets. We found that graphene sheets with different reduction levels can all form stable dispersions after amphiphilic functionalization (see section 2 in Supporting Information).

We demonstrated excellent solubility of mPEG-rGO as prepared in various solvents, which was very important for post-treatment process and potential functionalization of electrode materials^{27,29,30}. Fig. 2b shows the typical dispersions of the mPEG-rGO in water, DMF, ethanol, acetone, tetrahydrofuran (THF), and chloroform, at 1 mg/mL concentration. The black dispersion of mPEG-rGO in these solvents (except ethanol) contained no visible precipitate and was stable for weeks. A

control sample was synthesized under the same reaction condition, except that a tiny amount of mPEG molecules might be adsorbed on graphene surface by use of non-reactive pure mPEG 5k instead of A-mPEG 5k. The XRD pattern of the control demonstrated it was reduced as its 2θ peak was almost identical with that of mPEG-rGO (Supporting Information, Fig. S8). However, the vials with the control in all these solvents contained visible precipitates, indicating poor dispersion. The reason was that the covalent bonding of mPEG chain can facilitate the solubility of carbon plane in these solvents.

The electrochemical property of mPEG-rGO was evaluated by cyclic voltammetry using a potentiostat with three-electrode system. The rGO prepared by the conventional method of using hydrazine as a reducing agent (rGO_{N₂H₄}) was included in the experiments, providing additional information on the electrical properties of GO in the reduced formulation for comparison²⁵. Fig. 3a shows different cyclic voltammograms (CVs) at GO, rGO_{N₂H₄}, and mPEG-rGO modified GC electrodes with 1.0 mM $\text{K}_3\text{Fe}(\text{CN})_6$ in the presence of 0.1 M KCl. After being modified with GO, the anodic and cathodic peaks almost disappeared, consistent with the previous reports²⁰. It demonstrated that the presence of GO layer blocked the diffusion of $\text{Fe}(\text{CN})_6^{3-}$ into the film. For the rGO modified GC electrode, our experiments displayed well-shaped and repeatable CV curves. Significantly, at the mPEG-rGO modified GC electrode, the current density in the overall potential range increased significantly compared with that observed at rGO_{N₂H₄} modified GC electrode, which was a key parameter for potential applications in neural stimulation. The CVs of rGO in PBS buffer (Fig. 3b) verified that mPEG-rGO modified GC electrode can provide much stronger charge injection ability with the same geometrical area in the potential window ranging from -0.2 to $+0.8\text{ V}$.

It's notable that surface modification of graphene with biological molecules (e.g. PEG) often enhances the cell viability and functions for biomedicine applications³¹. The morphology of PC12 cells cultured on mPEG-rGO film was examined by scanning electron microscopy. Fig. S9 (Supporting Information) illustrated that PC12 cells formed a well-developed neural network and exhibited excellent cell adhesion on mPEG-rGO film. In addition, the cells exhibited polygonal or fusiform morphologies, suggesting good phenotypic spreading of PC12 cells on the mPEG-rGO film³². Cytotoxicity of mPEG-rGO was evaluated by Calcein-AM and EthD-I staining assay using LIVE/DEAD[®] Viability/Cytotoxicity Kit for mammalian cells (Invitrogen, USA), with TCPS as control. As shown in Fig. S10 (Supporting Information), nearly 90% of PC12 cells cultured on mPEG-rGO for 2 days were viable, while the cell viability difference between mPEG-rGO film and TCPS was neglectable (confirmed with MTT assay, Fig. S11 in Supporting Information). These data demonstrated good biocompatibility of mPEG-rGO, consistent with previous studies^{33,34}.

Right before electrical stimulation, PC12 neural cells on the rGOs were stained with Fluo-4 AM dye ($2.5\text{ }\mu\text{mol}$, Dojindo Laboratories, Japan). A series of $1\text{--}100\text{ ms}$ monophasic anodic pulses were administrated with durations of 10 s using a function generator (S3K, Grass Technologies, USA) and the stimulation threshold was 0.6 V ³⁵. Fig. 4a&b shows the fluorescence level of the PC12 cells on mPEG-rGO films increased during a stimulus,

whereas the intensity change on control film of rGO_{N2H4} was obscure. The relative change in fluorescence intensity $\Delta F/F$ was plotted versus stimulation time in Fig. 4c, the typical cells exhibited over 40–50% and 10–20% fluorescence intensity increase on mPEG-rGO and rGO_{N2H4} films via electrical stimuli, respectively. The cells with various $\Delta F/F$ changes were illustrated in Fig. S12 (Supporting Information), suggesting a threshold ($\Delta F/F > 5\%$) for fluorescent differentiable responses to electrical stimuli. The statistical histogram (Fig. 4d) showed that the percent of cell with large $\Delta F/F$ ($>5\%$) on mPEG-rGO was significantly higher than that on rGO_{N2H4} and indium tin oxide film (Fig. S13 in Supporting Information), indicating that the number of cells evoked a strong action potential on mPEG-rGO was tremendously increased even under the identical stimulation voltage (see Fig. S14 in Supporting Information for significance analysis). This evidence supported that amphiphilic mPEG-rGO performed better than rGO_{N2H4} as electrode materials. We proposed that mPEG-rGO should enable electrical stimulation of cells at higher current density owing to its elevated double-layer charging capacitance. In physiological solutions, the double layer at the electrode/electrolyte interface serves as the capacitor. According to equation $Q_{\max} = CV_{\max} = \epsilon_0 \epsilon_r (A/d) V_{\max}^2$, a reasonable approach to increase Q_{\max} is to increase relative permittivity (ϵ_r) which is contributed by the mPEG chains. On the other hand, the amphiphilic functionalization may increase the wettable surface area (A) accessible by electrolyte ions, giving rise to a much higher double-layer charging capacitance³⁶. As a result, mPEG-rGO electrode can provide an elevated current density, which played an important role in regulating cell behavior during electrical stimulation³⁷. These results promised effective electrode materials for neural research using amphiphilic mPEG-rGO as a conductive scaffold.

Conclusions

In summary, we demonstrated an effective thermal reduction method to prepare amphiphilic mPEG-rGO sheets for electrical stimulation of neural cells. Taking advantage of the amphiphilicity of mPEG, the functionalized rGO can well disperse in a variety of solvents, including chloroform and water. Measurements of cyclic voltammetry supported that amphiphilic mPEG-rGO modified electrode can provide much stronger charge injection ability than conventional rGO_{N2H4}. Furthermore, calcium image of PC12 cells verified that mPEG-rGO was an efficient conductive platform to mediate electrical stimulation for neural cells featured with an enhancement of double-layer charging capacitance. Importantly, amphiphilic functionalization in this novel graphene composite renders the good biocompatibility and high charge injection capability in the physiological environment, making it a promising platform for applications in neural prostheses and neural tissue engineering.

Acknowledgements

This work was supported by the Major State Basic Research Development Program (2013CB932702, 2012CB932601), and by NSFC (21275106) and NSF of Jiangsu Province (BK20130306); a project supported by the Priority Academic Program Development of Jiangsu Higher Education Institutions, and Open

Project Program of State Key Laboratory of Molecular Engineering of Polymers (Fudan University, K2012-09). J.L. was supported by the “Youth 1000-plan” in the Recruitment Program of Global Experts.

Notes and references

^a 199 Ren Ai Road, Soochow University, Suzhou Industrial Park, Jiangsu 215123, China. E-mail: jliu@suda.edu.cn
^c 398 Ruoshui Road, Suzhou Industrial Park, Jiangsu 215123, China. E-mail: gscheng2006@sinano.ac.cn

† Electronic Supplementary Information (ESI) available: [Activation of mPEG 5k, Preparation of reduced graphene oxides, FTIR, UV-Vis spectroscopy, XPS, Raman spectroscopy, TGA, XRD, Cell viability assay, Electrical stimulation of PC12 neural cells]. See DOI: 10.1039/b000000x/

- B. C. Thompson, R. T. Richardson, S. E. Moulton, A. J. Evans, S. O'Leary, G. M. Clark and G. G. Wallace, *J. Control. Release*, 2010, **141**, 161-167.
- N. A. Kotov, J. O. Winter, I. P. Clements, E. Jan, B. P. Timko, S. Campidelli, S. Pathak, A. Mazzatenta, C. M. Lieber, M. Prato, R. V. Bellamkonda, G. A. Silva, N. W. S. Kam, F. Patolsky and L. Ballerini, *Adv. Mater.*, 2009, **21**, 3970-4004.
- S. F. Cogan, *Annu. Rev. Biomed. Eng.*, 2008, **10**, 275-309.
- K. Wang, H. A. Fishman, H. Dai and J. S. Harris, *Nano Lett.*, 2006, **6**, 2043-2048.
- Y.-J. Huang, H.-C. Wu, N.-H. Tai and T.-W. Wang, *Small*, 2012, **8**, 2869-2877.
- B. Li, X. Cao, H. G. Ong, J. W. Cheah, X. Zhou, Z. Yin, H. Li, J. Wang, F. Boey, W. Huang and H. Zhang, *Adv. Mater.*, 2010, **22**, 3058-3061.
- C. Wang, L. Feng, H. Yang, G. Xin, W. Li, J. Zheng, W. Tian and X. Li, *Phys. Chem. Chem. Phys.*, 2012, **14**, 13233-13238.
- H. Dong, Z. Zhao, H. Wen, Y. Li, F. Guo, A. Shen, F. Pilger, C. Lin and D. Shi, *Sci. China Chem.*, 2010, **53**, 2265-2271.
- G. P. Keeley, A. O'Neill, M. Holzinger, S. Cosnier, J. N. Coleman and G. S. Duesberg, *Phys. Chem. Chem. Phys.*, 2011, **13**, 7747-7750.
- N. Li, X. Zhang, Q. Song, R. Su, Q. Zhang, T. Kong, L. Liu, G. Jin, M. Tang and G. Cheng, *Biomaterials*, 2011, **32**, 9374-9382.
- A. Bendali, L. H. Hess, M. Seifert, V. Forster, A.-F. Stephan, J. A. Garrido and S. Picaud, *Adv. Healthcare Mater.*, 2013, **2**, 929-933.
- T. R. Nayak, H. Andersen, V. S. Makam, C. Khaw, S. Bae, X. Xu, P.-L. R. Ee, J.-H. Ahn, B. H. Hong, G. Pastorin and B. Ozyilmaz, *ACS Nano*, 2011, **5**, 4670-4678.
- Y. Wang, W. C. Lee, K. K. Manga, P. K. Ang, J. Lu, Y. P. Liu, C. T. Lim and K. P. Loh, *Adv. Mater.*, 2012, **24**, 4285-4290.
- O. Akhavan and E. Ghaderi, *J. Mater. Chem. B*, 2013, **1**, 6291-6301.
- W. C. Lee, C. H. Y. X. Lim, H. Shi, L. A. L. Tang, Y. Wang, C. T. Lim and K. P. Loh, *ACS Nano*, 2011, **5**, 7334-7341.
- O. Akhavan, E. Ghaderi and M. Shahsavari, *Carbon*, 2013, **59**, 200-211.
- O. Akhavan, E. Ghaderi, E. Abouei, S. Hatamie and E. Ghasemi, *Carbon*, 2014, **66**, 395-406.
- C. Lee, X. Wei, J. W. Kysar and J. Hone, *Science*, 2008, **321**, 385-388.
- K. S. Kim, Y. Zhao, H. Jang, S. Y. Lee, J. M. Kim, K. S. Kim, J.-H. Ahn, P. Kim, J.-Y. Choi and B. H. Hong, *Nature*, 2009, **457**, 706-710.
- L. Chen, Y. Tang, K. Wang, C. Liu and S. Luo, *Electrochem. Commun.*, 2011, **13**, 133-137.
- S. Y. Park, J. Park, S. H. Sim, M. G. Sung, K. S. Kim, B. H. Hong and S. Hong, *Adv. Mater.*, 2011, **23**, H263-H267.

- 22 W. S. Hummers Jr and R. E. Offeman, *J. Am. Chem. Soc.*,
1958, **80**, 1339-1339.
- 23 S. Stankovich, D. A. Dikin, R. D. Piner, K. A. Kohlhaas, A.
Kleinhammes, Y. Jia, Y. Wu, S. T. Nguyen and R. S. Ruoff,
5 *Carbon*, 2007, **45**, 1558-1565.
- 24 H. Petersen, P. M. Fechner, D. Fischer and T. Kissel,
Macromolecules, 2002, **35**, 6867-6874.
- 25 D. Li, M. B. Muller, S. Gilje, R. B. Kaner and G. G. Wallace,
Nat. Nanotechnol., 2008, **3**, 101-105.
- 10 26 S. Stankovich, R. D. Piner, S. T. Nguyen and R. S. Ruoff,
Carbon, 2006, **44**, 3342-3347.
- 27 B. K. Ahn, J. Sung, Y. Li, N. Kim, M. Ikenberry, K. Hohn, N.
Mohanty, P. Nguyen, T. S. Sreeprasad, S. Kraft, V. Berry and
X. S. Sun, *Adv. Mater.*, 2012, **24**, 2123-2129.
- 15 28 X. Qi, K.-Y. Pu, H. Li, X. Zhou, S. Wu, Q.-L. Fan, B. Liu, F.
Boey, W. Huang and H. Zhang, *Angew. Chem. Int. Ed.*, 2010,
49, 9426-9429.
- 29 J. Shen, Y. Hu, C. Li, C. Qin and M. Ye, *Small*, 2009, **5**, 82-
85.
- 20 30 S. Stankovich, R. D. Piner, X. Chen, N. Wu, S. T. Nguyen and
R. S. Ruoff, *J. Mater. Chem.*, 2006, **16**, 155-158.
- 31 Y. Hernandez, V. Nicolosi, M. Lotya, F. M. Blighe, Z. Sun, S.
De, I. T. McGovern, B. Holland, M. Byrne, Y. K. Gun'Ko, J. J.
Boland, P. Niraj, G. Duesberg, S. Krishnamurthy, R. Goodhue,
25 J. Hutchison, V. Scardaci, A. C. Ferrari and J. N. Coleman,
Nat. Nanotechnol., 2008, **3**, 563-568.
- 32 Y. Liu, X. Liu, J. Chen, K. J. Gilmore and G. G. Wallace,
Chem. Commun., 2008, 3729-3731.
- 33 Y. Zhang, S. F. Ali, E. Dervishi, Y. Xu, Z. Li, D. Casciano and
A. S. Biris, *ACS Nano*, 2010, **4**, 3181-3186.
- 30 34 A. M. Pinto, S. Moreira, I. C. Gonçalves, F. M. Gama, A. M.
Mendes and F. D. Magalhães, *Colloids Surf. B: Biointerfaces*,
2013, **104**, 229-238.
- 35 N. Li, Q. Zhang, S. Gao, Q. Song, R. Huang, L. Wang, L. Liu,
J. Dai, M. Tang and G. Cheng, *Sci. Rep.*, 2013, **3**, 1604.
- 36 T. Y. Kim, H. W. Lee, M. Stoller, D. R. Dreyer, C. W.
Bielawski, R. S. Ruoff and K. S. Suh, *ACS Nano*, 2010, **5**,
436-442.
- 37 A. Kotwal and C. E. Schmidt, *Biomaterials*, 2001, **22**, 1055-
40 1064.

FIGURE CAPTIONS

Scheme 1. Preparation of mPEG-rGO film for electrical stimulation of PC12 neural cells. Step 1. Thermal reduction and functionalization of GO in the presence of A-mPEG 5K. Step 2: Electrical stimulation of PC12 cells on amphiphilic mPEG-rGO films.

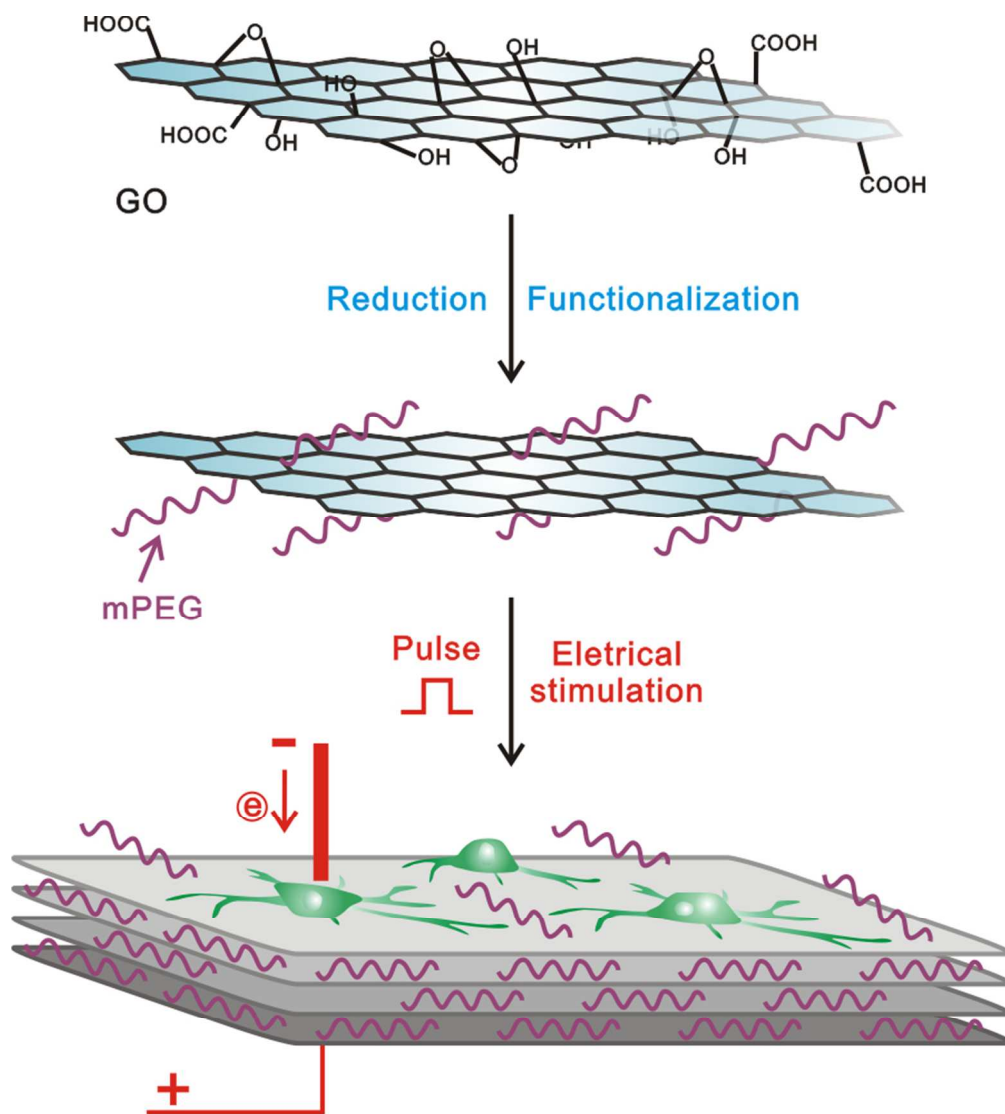
Figure 1. Tapping-mode AFM images and cross-sectional analysis of a) GO and b) mPEG-rGO on mica.

5 **Figure 2.** Characterization of mPEG-rGO. (a) XRD patterns of GO, mPEG-rGO obtained at 60, 80 and 160 °C, and rGO_{N₂H₄} (as benchmarks). (b) Photographs of mPEG-rGO (top) and the control (bottom) dispersed in various solvents. The concentrations of rGO and the control are ~1 mg/mL.

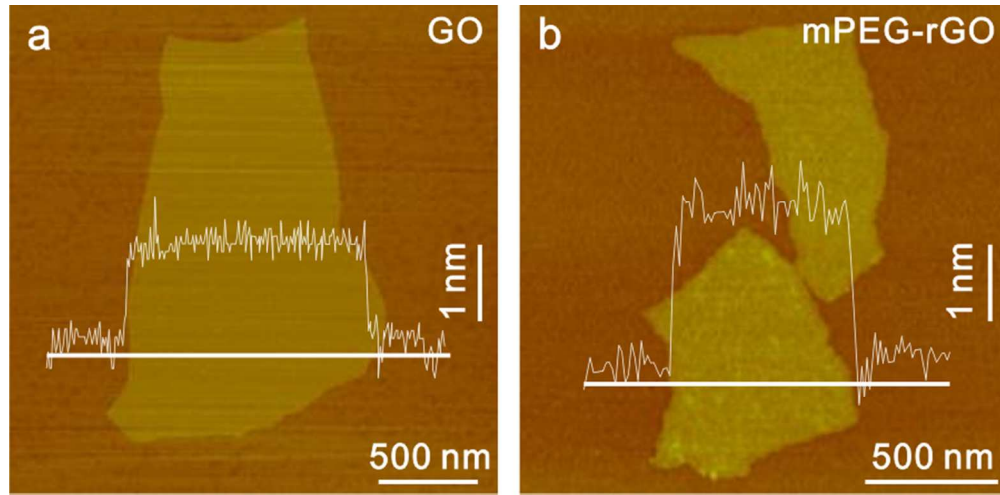
Figure 3. CVs recorded at GO/GC, rGO_{N₂H₄}/GC or mPEG-rGO/GC electrode with 1 mM K₃Fe(CN)₆ in the buffer of 0.1 M KCl (a) and with 1× PBS buffer (b), scan rate: 50 mV/s.

10 **Figure 4.** Electrical stimulation of PC12 cells on mPEG-rGO. Fluorescence imaging of the cells pre-incubated with Fluo-4 AM dye on mPEG-rGO (a) & rGO_{N₂H₄} (b) films before (left) and after (right) electrical stimulation. Panel (c) plots the relative fluorescence intensity change $\Delta F/F$ of the circled cell in panel (a&b) versus the stimulation time period. Histogram (d) depicts the percent of cells in the different range of $\Delta F/F$.

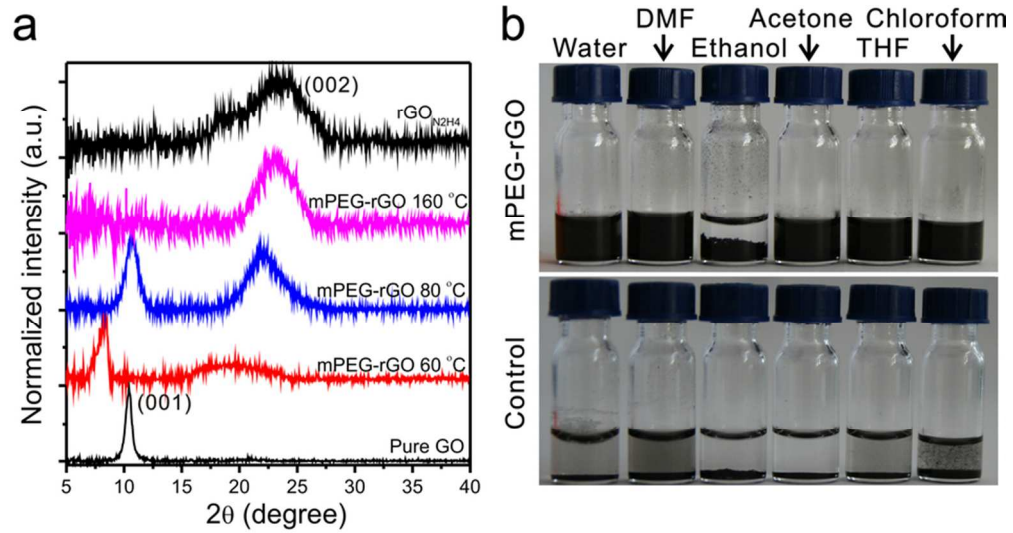
15



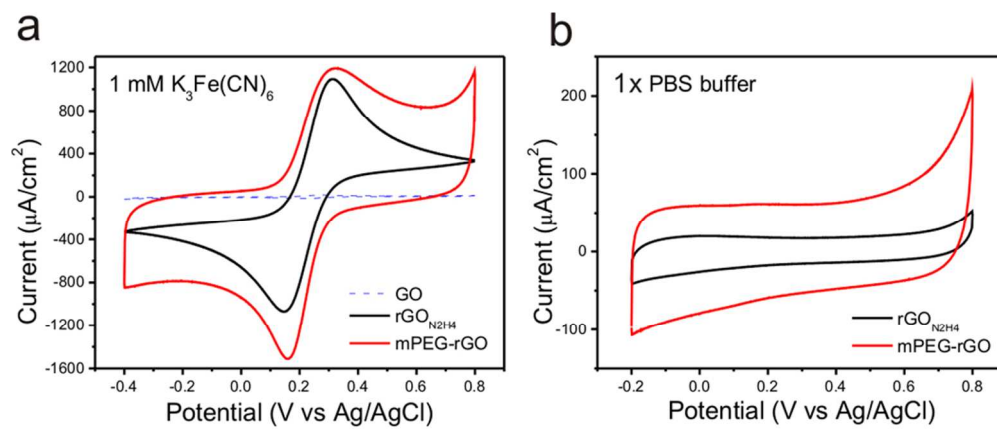
76x83mm (300 x 300 DPI)



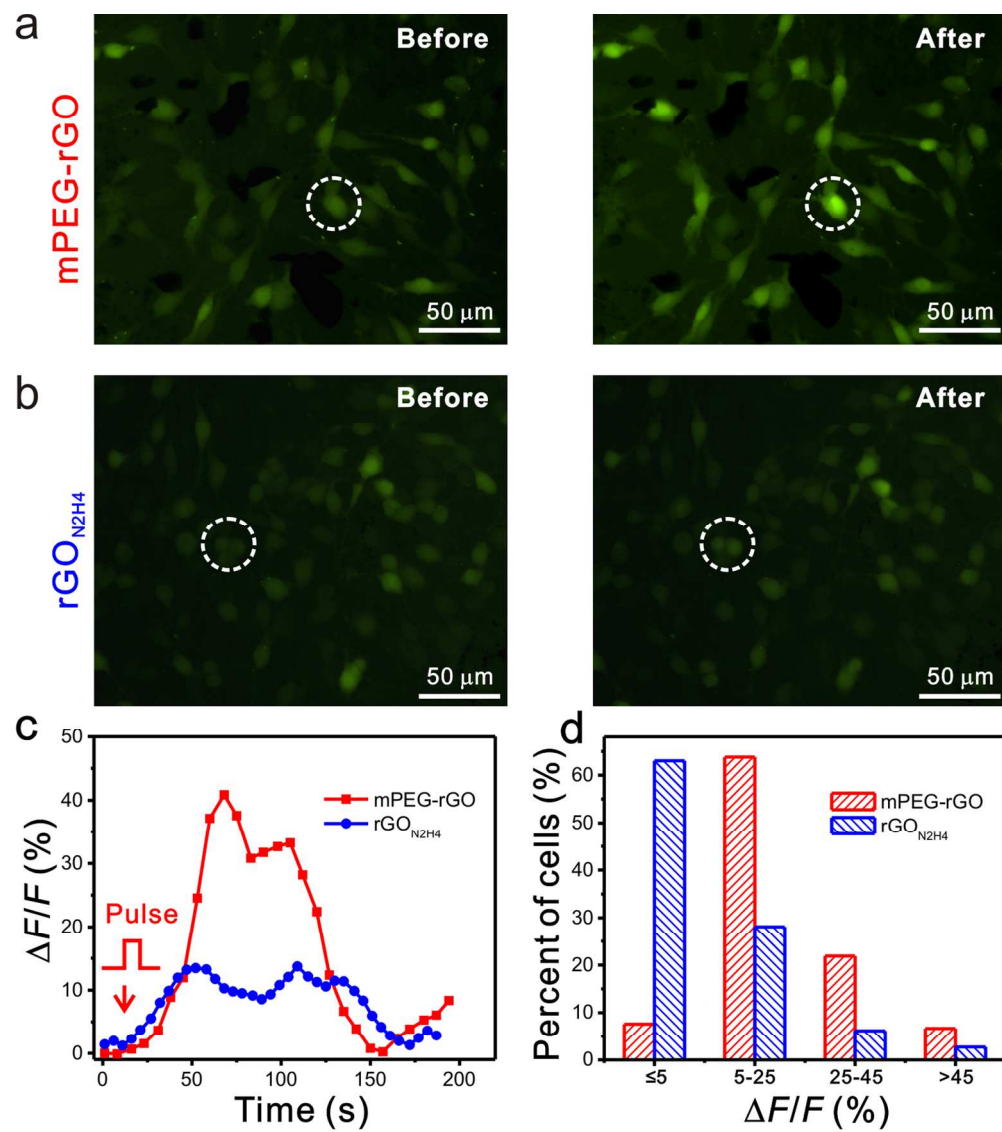
76x37mm (300 x 300 DPI)



80x42mm (300 x 300 DPI)

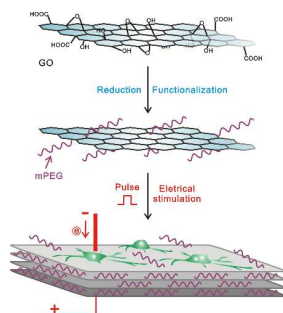


88x37mm (300 x 300 DPI)



152x170mm (300 x 300 DPI)

Graphic Abstract



A facile method was developed to synthesize amphiphilic reduced graphene oxide for electrical stimulation of neural cells with high charge injection capacity.